Cancer Letters 459 (2019) 204–215

Contents lists available at ScienceDirect

Cancer Letters

journal homepage: www.elsevier.com/locate/canlet

Original Articles

Macrophage-expressed CD51 promotes cancer stem cell properties via the TGF-β1/smad2/3 axis in pancreatic cancer

Bin Zhang[a,b,f,g,1], Huilin Ye[a,b,1], Xiaofan Ren[a,c,1], Shangyou Zheng[a,b], Quanbo Zhou[a,b], Changhao Chen[a,d], Qing Lin[a,b], Guolin Li[a,b], Lusheng Wei[a,b], Zhiqiang Fu[a,b], Yuting Zhang[e], Chonghui Hu[a,b], Zhihua Li[a,c,**,2], Rufu Chen[a,b,*,2]

[a] Guangdong Provincial Key Laboratory of Malignant Tumor Epigenetics and Gene Regulation, Sun Yat-sen Memorial Hospital, Sun Yat-sen University, Guangzhou, Guangdong Province, 510120, China
[b] Department of Pancreatobiliary Surgery, Sun Yat-sen Memorial Hospital, Sun Yat-sen University, Guangzhou, Guangdong Province, 510120, China
[c] Department of Medical Oncology, Sun Yat-sen Memorial Hospital, Sun Yat-sen University, Guangzhou, Guangdong Province, 510120, China
[d] Department of Urology, State Key Laboratory of Oncology in South China, Sun Yat-sen Memorial Hospital, Guangzhou, Guangdong Province, 510120, China
[e] Zhongshan School of Medicine, Sun Yat-sen University, Guangzhou, Guangdong Province, 510080, China
[f] Department of Colorectal Surgery, The Sixth Affiliated Hospital of Sun Yat-sen University, Guangzhou,Guangdong Province,510655, China
[g] Guangdong Provincial Key Laboratory of Colorectal and Pelvic Floor Diseases, The Sixth Affiliated Hospital of Sun Yat-sen University, Guangzhou, Guangdong Province, 510655, China

ARTICLE INFO

Keywords:
Pancreatic ductal adenocarcinoma
Cancer stem cell
Tumor-associated macrophage
Integrin
Biomarker

ABSTRACT

Macrophage-targeted therapy offers new options for intractable pancreatic ductal adenocarcinoma (PDAC), which has a low 5-year survival rate. However, the factors regulating the biological function and phenotype of macrophages in PDAC are incompletely understood. Here, we found that CD51 was positively associated with the poor prognosis of PDAC patients and was highly expressed on macrophages but not on pancreatic cancer cells. Subsequently, we found that CD51 was a marker of macrophages, which promoted the stemness of pancreatic cancer cells. Furthermore, knockdown of CD51 in macrophages drove macrophages toward an M1-like phenotype. Mechanistically, macrophage-expressed CD51 contributed to the acquisition of stemness traits of pancreatic cancer cells by regulating the TGF-β1/smad2/3 pathway. Our data demonstrate the central role played by macrophage-expressed CD51 in the acquisition of stemness traits of pancreatic cancer cells through the paracrine induction of TGF-β1. We first show the connection between the CD51/TGF-β1/smad2/3 axis and PDAC cancer stem cell properties and then indicate that CD51-targeted therapy is a new therapeutic modality for PDAC.

Abbreviations: PDAC, Pancreatic ductal adenocarcinoma; CSCs, Cancer stem cells; MDSCs, Myeloid-derived suppressor cells; TAMs, Tumor-associated macrophages; IHC, Immunohistochemistry; TCGA, The Cancer Genome Atlas; PSCs, Pancreatic stellate cells; KIRC, Kidney renal clear cell carcinoma; GBM, Glioblastoma multiforme; LGG, Brain lower grade glioma; ESCA, Esophageal carcinoma; THCA, Thyroid carcinoma; PAAD, Pancreatic adenocarcinoma; HNSC, Head and neck squamous cell carcinoma; LUSC, Lung squamous cell carcinoma; CHOL, Cholangiocarcinoma; KICH, Kidney chromophobe; BRCA, Breast invasive carcinoma; SARC, Sarcoma; LUAD, Lung adenocarcinoma; STAD, Stomach adenocarcinoma; CESC, Cervical squamous cell carcinoma and endocervical adenocarcinoma; SKCM, Skin cutaneous melanoma; KIRP, Kidney renal papillary cell carcinoma; PRAD, Prostate adenocarcinoma; READ, Rectal adenocarcinoma; BLCA, Bladder urothelial carcinoma; COAD, Colon adenocarcinoma; OV, Ovarian serous cystadenocarcinoma; PCPG, Pheochromocytoma and paraganglioma; UCEC, Uterine corpus endometrial carcinoma; UCS, Uterine carcinosarcoma; ACC, Adrenocortical carcinoma; THYM, Thymoma; LAML, Acute myeloid leukemia; TGCT, Testicular germ cell tumors; LIHC, Liver hepatocellular carcinoma; DLBC, Lymphoid neoplasm diffuse large B cell lymphoma

* Corresponding author. Guangdong Provincial Key Laboratory of Malignant Tumor Epigenetics and Gene Regulation, Sun Yat-sen Memorial Hospital, Sun Yat-sen University, Guangzhou, Guangdong Province, 510120, China.
** Corresponding author. Guangdong Provincial Key Laboratory of Malignant Tumor Epigenetics and Gene Regulation, Sun Yat-sen Memorial Hospital, Sun Yat-sen University, Guangzhou, Guangdong Province, 510120, China.
E-mail addresses: zhihuali_sysu@163.com (Z. Li), Chenrufu@mail.sysu.edu.com (R. Chen).
[1] These authors contributed equally: Bin Zhang, Huilin Ye, and Xiaofan Ren.
[2] Zhihua Li and Rufu Chen are co-corresponding authors.

https://doi.org/10.1016/j.canlet.2019.06.005
Received 10 January 2019; Received in revised form 1 June 2019; Accepted 10 June 2019

1. Introduction

Pancreatic ductal adenocarcinoma (PDAC) is currently the fourth leading cause of cancer-related death in developed countries [1]. The survival rate has not improved significantly over the past 30 years, and less than 5% of patients remain alive 5 years after diagnosis [2]. These alarming statistics are primarily due to the inherent chemoresistant nature and metastatic capacity of PDAC [3], which lead to the cachexia and death of patients [4]. Currently, these characteristics are universally accepted to be driven by a subpopulation of highly plastic "stem-like" cells within the tumor known as cancer stem cells (CSCs) [5]. Therefore, targeting CSCs might facilitate the development of inhibitors to eliminate CSC populations and lead to tumor eradication.

CD51, also known as integrin αV, heterodimerizes with β1, β3, β5, β6, and β8 integrins and plays various physiological roles in tumor development processes such as cell adhesion and migration [6]. Our previous research showed that CD51 is a marker of colorectal CSCs [7]. Moreover, accumulating evidence shows that CD51 in cancer cells is associated with cancer progression in some solid tumors [8,9]. However, little is known about whether CD51 and CSCs interact in pancreatic cancer.

Integrins play a critical role in regulating the biological function of macrophages, especially in the processes of macrophage polarization [10] and cell adhesion [11]. A key macrophage lipid kinase, PI3Kγ, inhibits antitumor immunity by promoting integrin α4 expression, which facilitates the immunosuppressive polarization of myeloid-derived suppressor cells (MDSCs) and tumor-associated macrophages (TAMs) [12,13]. Glioblastoma stem cells (GSCs) secrete the protein POSTN, a TAM attractant. POSTN recruits macrophages through αVβ3 integrin signaling, proving the relationship between GSCs and TAMs in GBM tumors [14]. However, whether CD51 drives macrophage polarization remains largely unknown.

Here, we reported that CD51 is positively associated with the poor prognosis of PDAC patients. Moreover, we provide the first report that overexpression of CD51 in macrophages potentiates the self-renewal ability of pancreatic cancer cells—the foundational characteristic of CSCs. However, knockdown of CD51 in macrophages reduces the tumorigenic and metastatic capacities of pancreatic cancer cells *in vivo*. Mechanistically, we demonstrated that inhibition of CD51 expression in macrophages effectively diminishes the stemness of pancreatic cancer cells through the TGF-β1/smad2/3 pathway. Taken together, these results indicate that CD51 could be a novel functional M2 macrophage marker, shedding new light on future applications for targeting CD51 in cancer therapy, particularly in therapies focused on reprogramming to eliminate the protumoral activity of TAMs.

2. Materials and methods

2.1. Patients and clinical sample

One hundred and six paired PDAC and noncancerous tissues were obtained from informed patients who underwent surgical resection of primary pancreatic cancer in our department from January 2013 to July 2018. Our protocol was approved by the hospital's Protection of Human Subjects Committee. The diagnosis of PDAC was confirmed consistently by professional pathologists. No patient received any preoperative chemotherapy or radiotherapy. All samples were immediately snap-frozen in liquid nitrogen and stored at −80 °C until further use. The detailed clinical pathologic characteristics of the patients are summarized in Table 1. The overall survival (OS) time was explicitly defined as the time interval beginning at the date of surgery and ending at the date of death or at the end of follow-up.

2.2. Cell lines and chemicals

Human PDAC cell lines (PANC-1, SW1990, AsPC-1, BxPC-3 and CFPAC-1), the immortal human pancreatic duct epithelial cell line (HPDE6-C7), and human THP-1 monocytes were purchased from the American Type Culture Collection (ATCC; Rockville, MD, USA). Cells were maintained in Dulbecco's modified Eagle's medium (DMEM, Invitrogen, Carlsbad, CA, USA) or RPMI 1640 medium (Invitrogen, Carlsbad, CA, USA) containing 10% fetal bovine serum (FBS, Invitrogen, Carlsbad, CA, USA) and 1% penicillin/streptomycin and cultured at 37 °C in humidified air with 5% CO_2.

Table 1
Clinicopathological correlation of CD51 expression in PDACs.

Variable		$CD51^{low}$(n = 53)	$CD51^{high}$(n = 53)	P-value
Sex	Female	25	33	
	Male	28	20	0.1185
Age	≥60	28	22	
	< 60	25	31	0.0213*
AJCC stage	I	18	8	
	II	35	45	0.0240*
Tumor stage	T1	14	5	
	T2	17	12	
	T3	22	36	0.0142*
Lymph node stage	N0	23	37	
	N1	30	16	< 0.01*
Differentiation	Well	12	6	
	Moderate	38	38	
	Poor	3	9	0.0821
Neural invasion	Negative	24	28	
	positive	29	25	0.4371

AJCC American Joint Committee on Cancer.
*Denotes statistical significance.
P-values were calculated by Pearson Chi-square test.

2.3. RNA extraction and qRT-PCR

Total RNA was extracted using TRIzol reagent (Invitrogen, Carlsbad, CA, USA) according to the manufacturer's instructions. Total RNA was reverse transcribed to cDNA using a QuantiTect Reverse Transcription kit (Qiagen, Valencia, CA, USA), as described by the manufacturer. Quantitative polymerase chain reaction (qPCR) was performed using SYBR Green qPCR SuperMix (Roche, Basel, Switzerland) and a Light Cycler 480 Detection System (Roche, Basel, Switzerland). DNA was amplified using the following thermal cycling conditions: 40 cycles of denaturation at 95 °C for 10 s, annealing at 60 °C for 10 s, and extension at 72 °C for 30 s mRNA levels were normalized to those of β-actin or GAPDH. The primer sequences used for real-time PCR are listed in Supplementary Table 1.

2.4. Cell transfection and viral infection

Lentiviral-mediated shRNA interference was performed as described previously [7]. CD51 expression was knocked down in PDAC cell lines by transduction of a lentiviral vector. Lentiviruses were obtained by transfection of 293T cells. The PDAC cell lines were seeded into 6-well plates and transfected with CD51 shRNA using X-tremeGENE HP reagent (Roche Basel, Switzerland). Before the experiments, GFP-positive cells were isolated by flow cytometry. The knockdown efficacy of each shRNA-expressing lentivirus was assessed after 3 days by western blotting to explore the effects of CD51 knockdown on the PDAC cell lines or macrophages.

2.5. Cell proliferation and cell apoptosis assays

Cell viability was determined using a Cell Counting Kit-8 (CCK-8) assay kit. PDAC cells were plated at a density of 2×10^4 cells/ml in 96-well plates in culture medium (100 μl/well). After 4 h, 10 μl of CCK-8 solution was added to the cells in 96-well plates and incubated at 37 °C for 0.5–4 h. The spectral absorbance in each well was quantified at

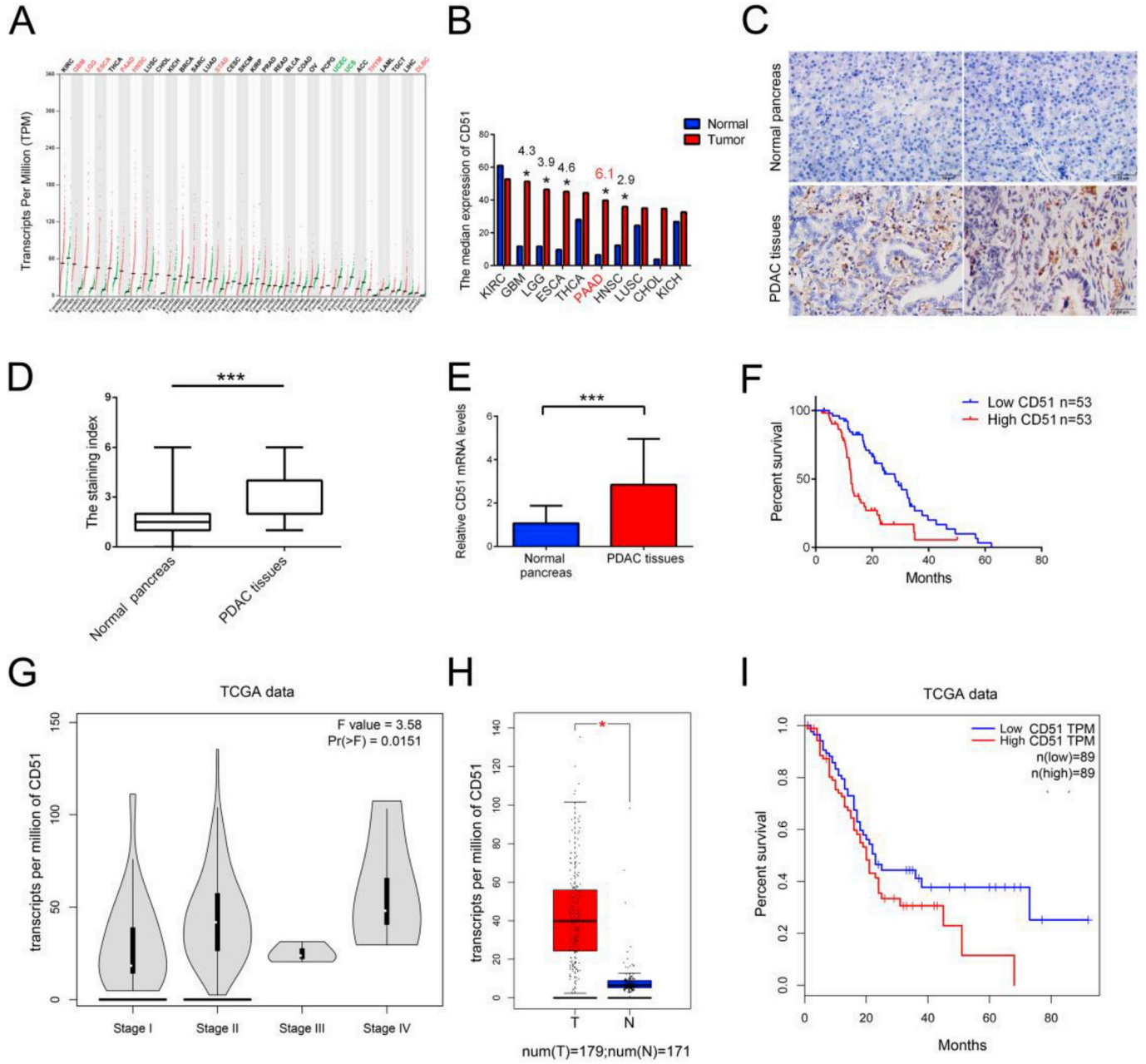

Fig. 1. High CD51 expression in human pancreatic cancer accelerates pancreatic cancer progression.

A. CD51 expression profile across all tumor samples and paired normal tissues. A red abbreviation represents significant upregulation in tumor tissues, while a green abbreviation represents significant downregulation in tumor tissues. The RNA sequencing expression data were obtained from the TCGA database and the Genotype–Tissue Expression (GTEx) project and were analyzed by the Gene Expression Profiling Interactive Analysis (GEPIA) tool.

B. CD51 expression profile across 10 tumor samples with high CD51 expression and the paired normal tissues. The height of the bars represents the median expression level in the indicated tumor types or normal tissues. The numbers above the bars are the ratios of the median expression level in the tumor tissue to that in the normal tissue (*P $<$ 0.05).

C. The immunohistochemistry (IHC) results showed that CD51 expression was higher in human PDAC tissues than in normal human pancreatic tissues.

D. CD51 staining intensities in human PDAC and normal human pancreatic tissues. The definition of the staining index is included in the "Materials and methods" section (***P $<$ 0.001).

E. qRT-PCR analysis of 106 PDAC samples and paired normal tissues (***P $<$ 0.001).

F. Kaplan–Meier survival analysis was performed by comparing CD51-high (n = 53) and CD51-low PDAC patients from Sun Yat-sen Memorial Hospital (n = 53) (P $<$ 0.01, log–rank test).

G. Transcripts per million mapped reads of CD51 in human pancreatic cancer samples from stage I to stage IV. The RNA sequencing expression data were obtained from the TCGA database and the GTEx project and were analyzed by the GEPIA tool (P = 0.0151, n = 179).

H. The CD51 expression profile in human pancreatic cancer samples and paired normal tissues was analyzed by the GEPIA tool using data from the TCGA database and the GTEx project (*P $<$ 0.05).

I. Kaplan–Meier survival analysis was performed by comparing CD51-high pancreatic cancers (n = 89) and CD51-low pancreatic cancers (n = 89) using the GEPIA tool.

Table 2
Univariate and multivariate analysis of Overall Survival (OS) in PDAC patients (n = 106).

Variables	Univariate analysis			Multivariate analysis		
	HR	95%CI	p-Value	HR	95%CI	p-Value
Sex	0.985	0.622–1.562	0.95			
Age	0.939	0.595–1.481	0.787			
Differentiation (Well vs. Moderate or Poor)	1.012	0.565–1.813	0.968			
Neural invasion	1.074	0.681–1.692	0.759			
Lymph node stage (N1 vs. N0)	1.565	0.970–2.525	0.066			
AJCC stage (II vs. I)	2.265	1.316–3.900	0.003**	2.095	1.031–4.255	0.041*
Tumor stage (T3 vs. T2 or T1)	1.597	1.010–2.524	0.045*	0.776	0.425–1.416	0.409
CD51 expression(High vs. low)	2.568	1.596–4.131	0.001**	2.219	1.338–3.683	0.002**

Abbreviations: HR = hazard ratio; 95%CI = 95% confidence interval; Cox regression analysis, * $P < 0.05$, ** $P < 0.01$.

450 nm using a microplate reader (Tecan Trading AG, Switzerland). Cell viability was calculated according to the manufacturer's instructions. At least 3 experiments were performed, with each condition tested in triplicate.

For the cell apoptosis assays, PANC-1 and SW1990 cells were harvested and stained in binding buffer with propidium iodide (PI) and fluorescein isothiocyanate (FITC)-conjugated Annexin V (BIOSCI BIOTECH, Shanghai, China) to detect the population of apoptotic cells. Annexin V-FITC and PI were added to a mixture containing 100 μL each of resuspended cells and binding buffer. After 15 min at room temperature, cells were washed and resuspended in binding buffer. Samples were analyzed and sorted on a BD Influx (BD Biosciences, New Jersey, USA); data were analyzed using FlowJo software.

2.6. Wound healing and transwell assays

PDAC cells were incubated in 6-well plates. When the cells reached 85% confluency, 10-μl sterile pipette tips were used to scratch the cell layer, and the cells were then cultured with medium containing 1% FBS for 48 h. At 2 different time points (0 h and 24 h), images of the plates were acquired using a microscope.

Migration assays were performed in 24-well plates according to the manufacturer's instructions using Millicell culture plate inserts (Millipore, Darmstadt, Germany). Briefly, 2×10^4 cells were added to the top chamber, and 10% FBS in DMEM was added to the bottom chamber as a chemoattractant. After 48 h of incubation at 37 °C, the cells that invaded through the membrane (migrated cells) were counted in 3 fields under a 200 × objective lens.

2.7. Time-lapse cell motility assay

The migration of cancer cells was monitored over 6 h using a Zeiss Axio Observer Z1 microscope (Zeiss, Pleasanton, CA, USA). Cells were cultured at 37 °C in an enclosed chamber containing a controlled proportion of CO_2. Cell migration was quantified once every 20 min for 6 h using computer-assisted tracking. The migration distances of individual cells were determined and analyzed.

2.8. THP-1 cell differentiation and polarization

To assess the differentiation and polarization of human THP-1 monocytes, THP-1 monocytes were treated with 10 ng/ml phorbol-12-myristate-13-acetate (PMA, Sigma, SaintLouis, Missouri, USA) for 24 h, followed by 20 ng/ml interleukin (IL) 4 and 20 ng/ml IL13 (Peprotech, New Jersey, USA) for 48 h to obtain M2-polarized macrophages. Alternatively, PMA-treated THP-1 cells were incubated with 15 ng/ml lipopolysaccharide (LPS, Peprotech, New Jersey, USA) for 48 h to obtain M1-polarized macrophages.

2.9. Tumor formation assay in the NOD/SCID mouse model

NOD/SCID mice (4-6 weeks old) were purchased and maintained at the Laboratory Animal Center of Sun Yat-sen University in a specific pathogen-free environment. The animal care and experimental protocols were approved by the Institutional Guidelines of Guangdong Province and by the Use Committee for Animal Care. Tumor formation was induced in NOD/SCID mice by the injection of 5×10^5 pancreatic cancer cells alone or mixed with 5×10^5 M2 macrophages. Tumor volumes were calculated using the following formula: $V = (L \times W^2)/2$ (V, volume; L, long axis diameter; W, short axis diameter). Xenograft sections (5-μm thick) were stained with hematoxylin and eosin (H&E). Mice were monitored for 8 weeks, and the incidence of tumor formation was examined. Animals that were injected with tumor cells but showed no sign of tumor burden were generally killed; animals were checked at the injection sites to confirm the absence of tumors.

2.10. Flow cytometry

Cells were analyzed by multicolor flow cytometry using a BD FACScan flow cytometer (BD, New Jersey, USA) and FlowJo software. Matched isotype controls were used as the negative control for all fluorescence-activated cell sorting (FACS) analyses and sorting. The antibodies used are shown in Supplemental Table 2. Cells were collected and mixed with the antibodies. After incubation in the dark for 30 min at 4 °C, cells were washed and resuspended in PBS to finish FACS analysis.

2.11. Immunofluorescence (IF) analysis

For immunofluorescence analysis, cells were fixed in 3.7% formaldehyde and permeabilized in 0.1% Triton X-100. After incubation with primary antibody followed by secondary antibody in the dark, cell nuclei were stained by incubation with 4′,6-diamidino-2-phenylindole (DAPI). Images were acquired at room temperature using an LSM710 confocal microscope (Zeiss, Pleasanton, CA, USA). The primary and secondary antibodies used are listed in Supplementary Table 2.

2.12. Western blot analysis

For the western blot assay, protein was separated by sodium dodecyl sulfate–polyacrylamide gel electrophoresis and transferred to a polyvinylidene difluoride membrane. After blocking, immunodetection was performed using primary and horseradish peroxidase-labeled secondary antibodies, followed by detection with enhanced chemiluminescence.

2.13. Immunohistochemistry (IHC)

Formalin-fixed, paraffin-embedded tissues were subjected to antigen retrieval in citrate buffer for 15 min. Sections were blocked in normal goat serum for 30 min and incubated with primary antibody at

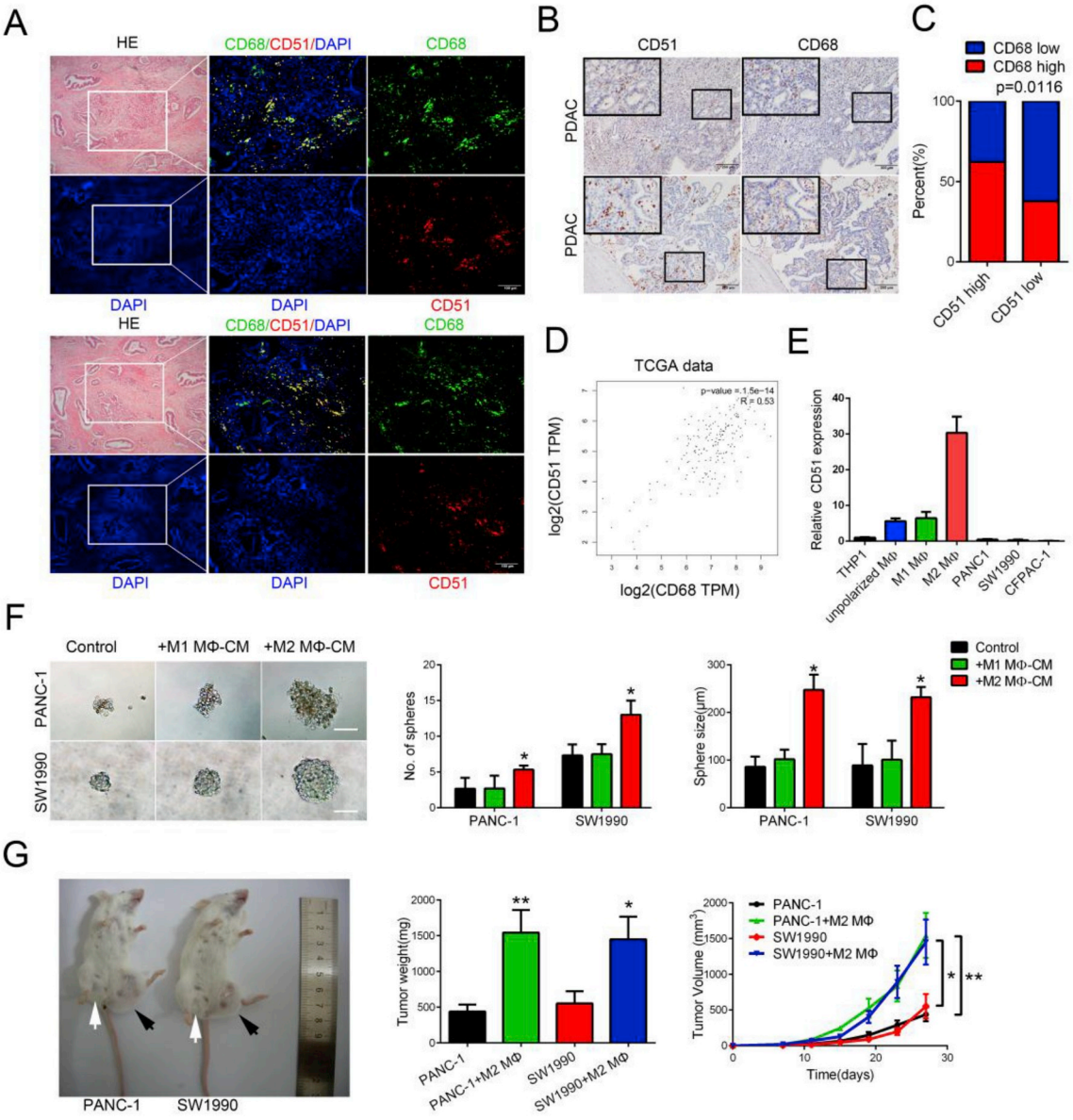

Fig. 2. CD51 is a marker of TAMs, which promote the stemness of pancreatic cancer cells.

A. Representative images of immunofluorescence results for anti-CD51 (red) and CD68 (green) staining on serial sections show that CD51 and CD68 were coexpressed in human pancreatic cancer.

B. Representative images of immunohistochemistry (IHC) on serial sections show that CD51 and CD68 (a macrophage marker) were coexpressed in human pancreatic cancer.

C. The percentage of CD68-high or CD68-low pancreatic cancer cells among CD51-high or CD51-low pancreatic cancer cell populations, respectively, were shown (chi-square test, P = 0.0116).

D. The correlation between CD51 and CD68 expression in the TCGA data was analyzed by the GEPIA tool (P = 1.5e-14).

E. Relative CD51 expression levels in macrophages and 3 pancreatic cancer cell lines were shown.

F. Sphere formation assays showed that PANC-1 and SW1990 cells cocultured with CM from M2 macrophages exhibited enhanced sphere-forming capacity. Scale bar, 100 μm (*P < 0.05).

G. Tumor formation was induced in NOD/SCID mice by injection with 5×10^5 pancreatic cancer cells alone or mixed with 5×10^5 M2 macrophages. Mice were randomized into 4 groups. The right sides of the mice were injected with pancreatic cancer cells (white arrow), while the left sides were injected with pancreatic cancer cells mixed with M2 macrophages (black arrow) (*: P < 0.05,**: P < 0.01).

4 °C overnight. Avidin–biotin peroxidase detection systems with DAB substrate were used to mark the locations of antigens. Then, nuclei were counterstained with hematoxylin. Immunohistochemically stained tumor sections were examined and scored independently by 2 observers for positively stained cells and immunohistochemical signal intensity as described previously [7].

2.14. Enzyme-linked immunosorbent assay (ELISA)

Cell culture supernatant was collected, and secreted TGF-β1 was quantified using a Human TGF-β1 ELISA Kit from Abcam (ab100647) according to the manufacturer's instructions. Briefly, the standards or samples were added to each well. The plate was then incubated and washed, and biotin-conjugated anti-TGF-β1 antibody was added to the appropriate wells. Then, the prepared streptavidin solution was added

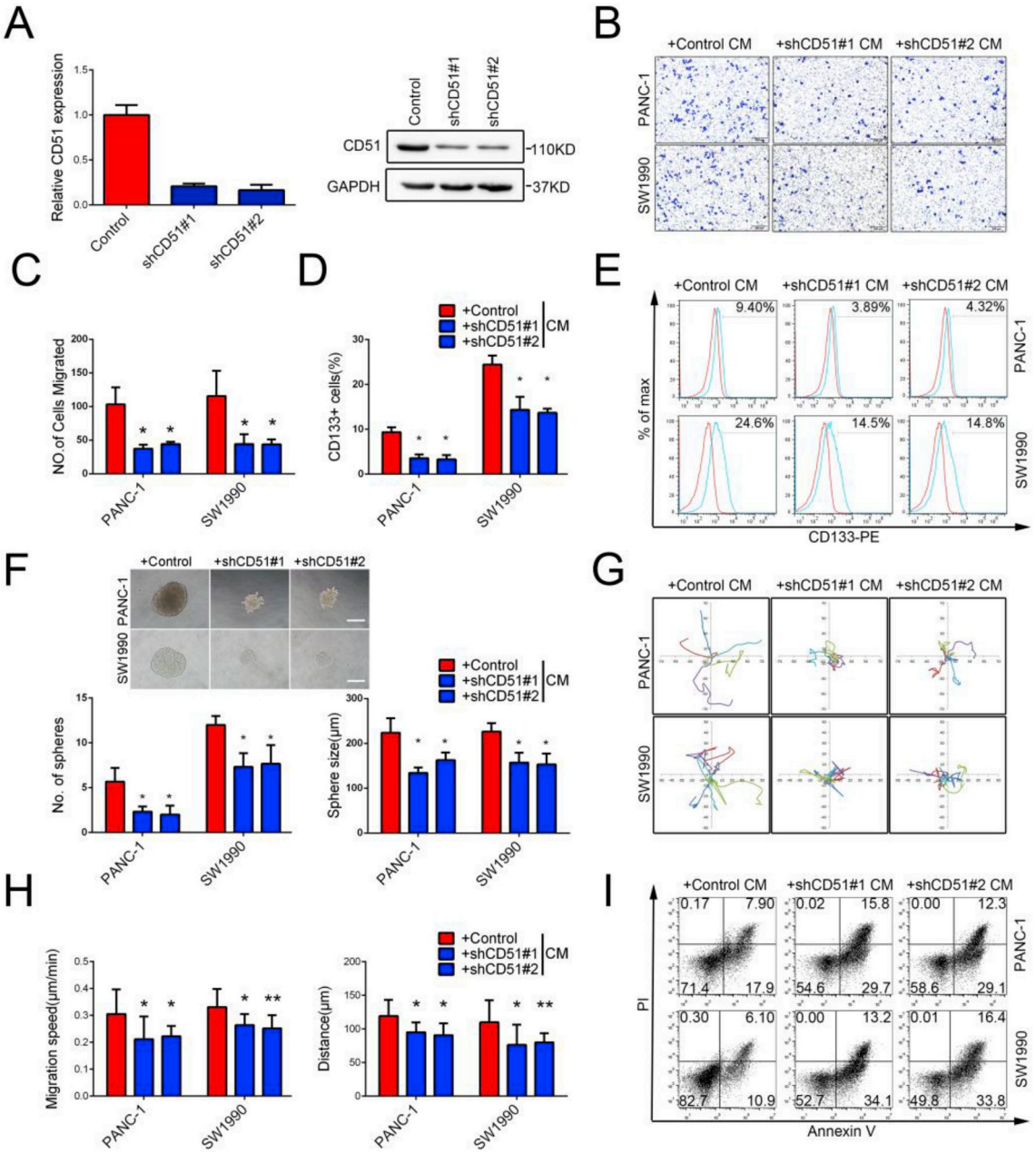

Fig. 3. Macrophage-expressed CD51 promotes CSC phenotypes in pancreatic cancer.

A. qRT-PCR and western blotting were performed to verify the knockdown of CD51 in M2 macrophages treated with CD51 shRNA.

B-C. Single-cell suspensions of PANC-1 and SW1990 pancreatic cancer cells were cocultured with control CM or CM from macrophages treated with CD51 shRNA. Representative images of the migration assay results were shown (*: $P < 0.05$).

D-E. Single-cell suspensions of PANC-1 and SW1990 pancreatic cancer cells were cocultured with control CM or CM from macrophages with CD51 knockdown. The ratios of CD133 + cells to total cells were analyzed (*: $P < 0.05$).

F. Sphere formation assays of pancreatic cancer cells cultured with macrophages as indicated (*: $P < 0.05$).

G-H. The motility of pancreatic cancer cells cultured with macrophages as indicated was assessed (*: $P < 0.05$, **: $P < 0.01$).

I. Gemcitabine was added to the media of PANC-1 and SW1990 cells cultured with macrophages as indicated. Apoptosis and necrosis were detected by flow cytometry using Annexin V-FITC and PI.

to the appropriate wells. TMB substrate was then added to each well. Finally, stop solution was added to each well. Plates were read at 450 nm immediately.

2.15. Sphere formation assay

PANC-1 and SW1990 cells were plated in 96-well ultra-low attachment plates (Corning, Corning, NY, USA) at a density of 1,000 viable cells per well. Cells were grown in standard sphere-forming medium (serum-free DMEM/F-12 supplemented with 1 × B27 serum substitute, 20 ng/ml human recombinant epidermal growth factor and 20 ng/ml basic fibroblast growth factor; all from Invitrogen, Carlsbad, CA, USA). Plates were incubated at 37 °C in 5% CO_2 for 14 days. Wells with spheres larger than 50 μm in diameter were counted.

2.16. Statistical analysis

All data are expressed as the means ± standard deviations (SDs) of

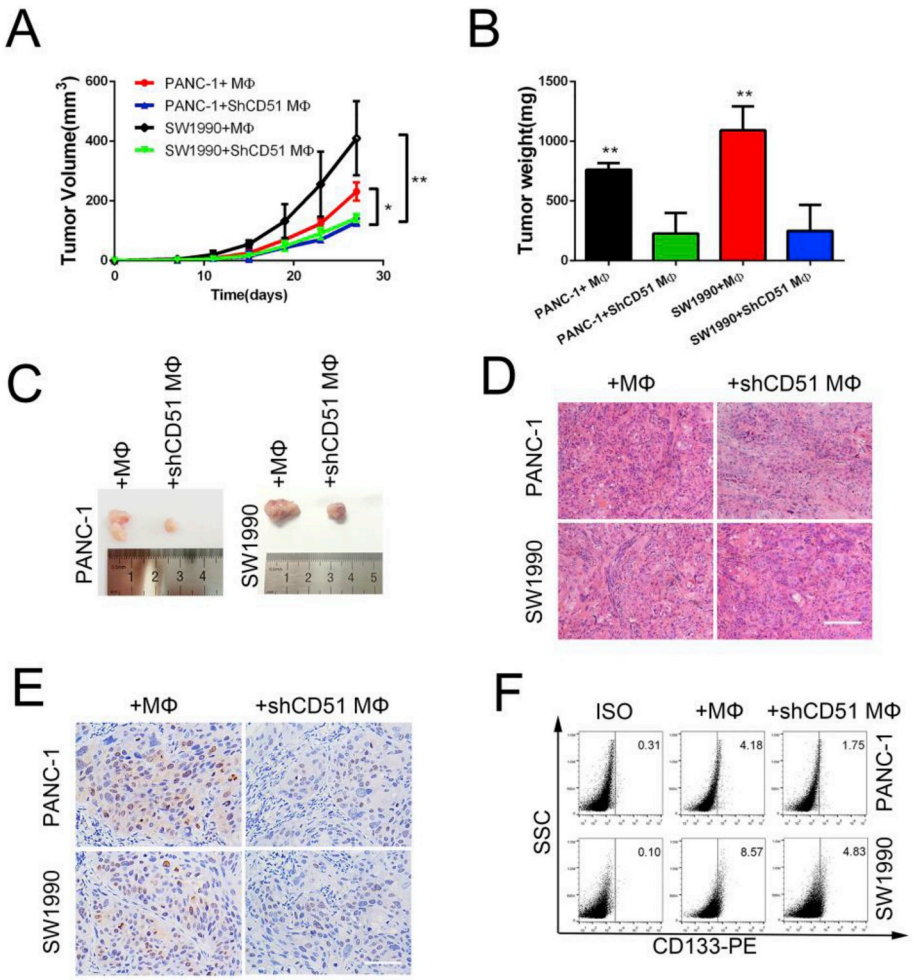

Fig. 4. CD51 knockdown in macrophages protects against pancreatic cancer.

A. Tumor formation was induced in NOD/SCID mice by the injection of pancreatic cancer cells mixed with the indicated macrophages. Tumor volumes were assessed (*: $P < 0.05$, **: $P < 0.01$).

B. Tumor formation was induced in NOD/SCID mice by the injection of pancreatic cancer cells alone or mixed with the indicated macrophages. Tumor weights were assessed (**: $P < 0.01$).

C. Tumor formation was induced in NOD/SCID mice by the injection of pancreatic cancer cells alone or mixed with the indicated macrophages. Representative images of the tumors are shown.

D. Representative images of H&E-stained tumor sections were shown. Tumors formed from pancreatic cancer cells mixed with macrophages exhibited more mesenchyme than tumors formed from macrophages with CD51 knockdown. Scale bar = 100 μm.

E. Representative images of ki67-stained tumor sections were shown. Scale bar = 50 μm.

F. CD133 expression in tumors from mice was shown.

at least three independent experiments. Comparisons between groups were performed using one-way analysis of variance (ANOVA) or Student's *t*-test. Survival was measured according to the Kaplan–Meier method and analyzed by the log–rank test. The associations between clinicopathological characteristics and CD51 expression were analyzed using the $\chi 2$ test. If the sample size was less than 40 or the expected frequency was less than 1, correction was performed using the Fisher test. SPSS 19.0 (SPSS, Chicago, Illinois, USA) was used for all analyses. A two-sided P-value of < 0.05 was considered statistically significant.

3. Results

3.1. CD51 is upregulated in pancreatic cancer tissues and is associated with poor prognosis

Analysis of The Cancer Genome Atlas (TCGA) database [15] showed that among 31 types of tumors, CD51 expression was significantly different in 10 types of tumors compared with that in the corresponding normal tissues (Fig. 1A). Among the top 10 tumors with significantly different CD51 expression, the maximum ratio of the median CD51 expression in the tumor to that in normal tissues was 6.1 in pancreatic cancer (Fig. 1B). Additionally, we performed qRT-PCR and IHC on PDAC and normal adjacent tissues and found that CD51 was appreciably overexpressed in the pancreatic cancer tissues relative to that in the adjacent normal tissues (Fig. 1C–E). Moreover, statistical analysis demonstrated that the CD51 expression level in patients was correlated with age, tumor stage and lymph node metastasis (Table 1). Moreover, univariate and multivariate analyses demonstrated that AJCC stage and CD51 expression were independent prognostic factors (Table 2). Furthermore, Kaplan–Meier analysis showed that higher CD51 expression levels were correlated with shorter OS times in patients with PDAC (Fig. 1F). These results were further confirmed by analyses of the TCGA database, collectively supporting the oncogenic role of CD51 (Fig. 1G–I).

3.2. CD51 does not directly influence pancreatic cancer cells

We investigated whether CD51 affects pancreatic cancer cells and found by qRT-PCR that CD51 was overexpressed in the pancreatic ductal epithelial cell line HPDE6-C7 but not in the other 5 pancreatic cancer cell lines (Supplementary Fig. 1A), contradictory to previous conclusions that CD51 is upregulated in pancreatic cancer tissues. Considering that CD51 expression was associated with pancreatic cancer progression, two CD51-targeting short hairpin RNA (shRNA) sequences and expression plasmids were transfected into PANC-1 and SW1990 cells, respectively, for further functional analysis *in vitro*. The transfection efficiency of the CD51 shRNA constructs and overexpression plasmids was measured by qRT-PCR (Supplementary Fig. 1B, G). The CCK-8 and wound healing assay results demonstrated that tumor cell proliferation and migration were not affected by either downregulation or overexpression of CD51 (Supplementary Fig. 1C-E, H; Supplementary Fig. 2C). Similarly, the motility of PDAC cells showed the same results as seen in the wound healing assays (Supplementary Fig. 2A and B). In addition, the PANC-1 and SW1990 cell lines were treated with gemcitabine to evaluate the effect of CD51 on drug resistance in PDAC. As shown in Supplementary Fig. 1F and I, CD51 did not influence the gemcitabine sensitivity of these PDAC cells. Collectively, these results indicate that CD51 did not directly influence the

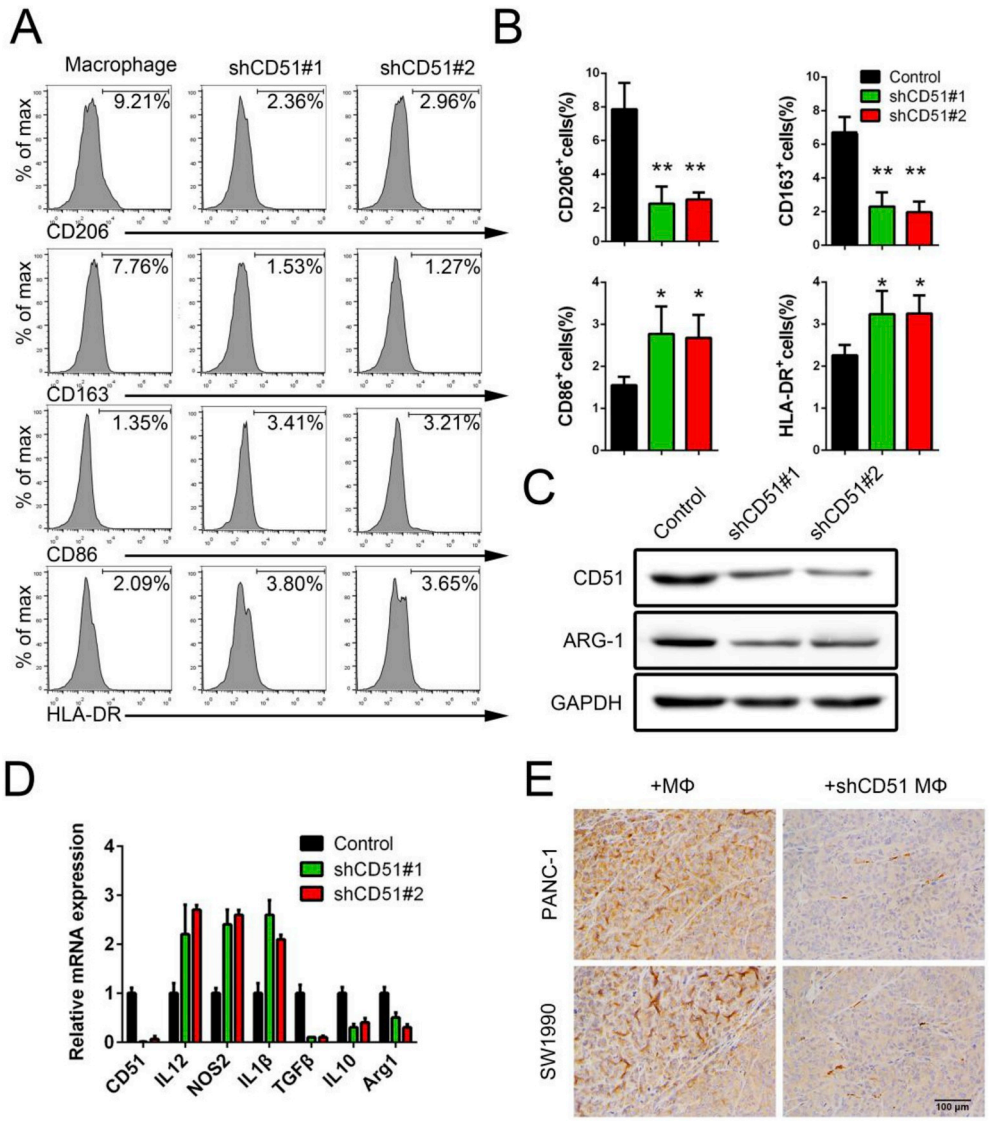

Fig. 5. CD51 drives macrophage polarization toward an M2-like phenotype.
A-B. Macrophages were gated and assessed for the expression of CD206 (an M2 marker), CD163 (an M2 marker), CD86 (an M1 marker), and HLA-DR (an M1 marker) (*: $P < 0.05$, **: $P < 0.01$).
C. Macrophages were subjected to western blot analysis with anti-arginase-1, anti-CD51, and anti-GAPDH antibodies.
D. Macrophages were assessed by qRT-PCR for the expression of IL-12, NOS2, IL1β, TGFβ1, IL10, and Arg1 as markers for M1 or M2 macrophages.
E. After the injection of mice with pancreatic cancer cells mixed with the indicated macrophages, xenograft sections were stained for arginase-1.

malignant biological behavior of PDAC cells.

3.3. CD51 is a marker of TAMs, which promote CSC properties

Although CD51 was positively associated with the poor prognosis of PDAC patients, it did not directly affect pancreatic cancer cells. We focused on peritumoral macrophages, a vital type of the most dynamic stromal cells in pancreatic cancer. We examined the expression of CD68 (a pan-macrophage marker) [16] and CD51 by staining sections of human pancreatic cancer tissues (Fig. 2A–C; Supplementary Fig. 3A and B). As expected, CD51 and CD68 were coexpressed in PDAC tissues, consistent with the correlation in the TCGA data (Fig. 2D). Macrophages can polarize into classically activated macrophage (M1) and alternatively activated macrophage (M2) phenotypes [17], which can be generated *in vitro* by differentiating and polarizing monocytic THP-1 cells through treatment with specific cytokines (Supplementary Fig. 4A-C). Subsequently, flow cytometric analysis was performed to further assess the expression of M2-specific (CD206 and CD163) and M1-specific (HLA-DR and CD86) markers (Supplementary Fig. 4D). Compared with pancreatic cancer cells, M2-like macrophages exhibited high CD51 expression (Fig. 2E). These results reveal a potential interaction between CD51 expression and TAMs.

Previous studies have reported that CSC properties can be promoted by microenvironmental factors in other solid tumors [18,19]. We aimed to investigate whether macrophages could also enhance CSC phenotypes in PDAC. Therefore, we examined the effects of both M1 and M2 macrophages on CSC phenotypes in PDAC. Compared with PDAC cells incubated with conditioned medium (CM) from M1 macrophages, PDAC cells incubated with CM derived from M2 macrophages had significantly increased mRNA levels of stemness-related genes (Supplementary Fig. 3C). In addition, when PDAC cells were cultured with CM from M2 macrophages, the sphere formation ability exhibited the largest increase (Fig. 2F). Consistent with the *in vitro* results, the results from the subcutaneous tumor model showed that tumor growth was significantly accelerated when PDAC cells were coinjected with M2 macrophages compared with that in the groups injected with pancreatic cancer cells alone (Fig. 2G). These data indicate that TAMs promote the stemness of pancreatic cancer cells.

3.4. Macrophage-expressed CD51 promotes CSC phenotypes in pancreatic cancer

To determine whether macrophage-expressed CD51 affects PDAC tumor growth, we interfered with CD51 expression by transfecting cells with shRNA#1 and shRNA#2 and comparing the resulting tumor growth with that of cells transfected with the negative control (NC) (Fig. 3A). Stemness-related genes (Nanog, Sox2, Oct3/4, KLF4, CD133 and CD24) in pancreatic cancer were downregulated in response to

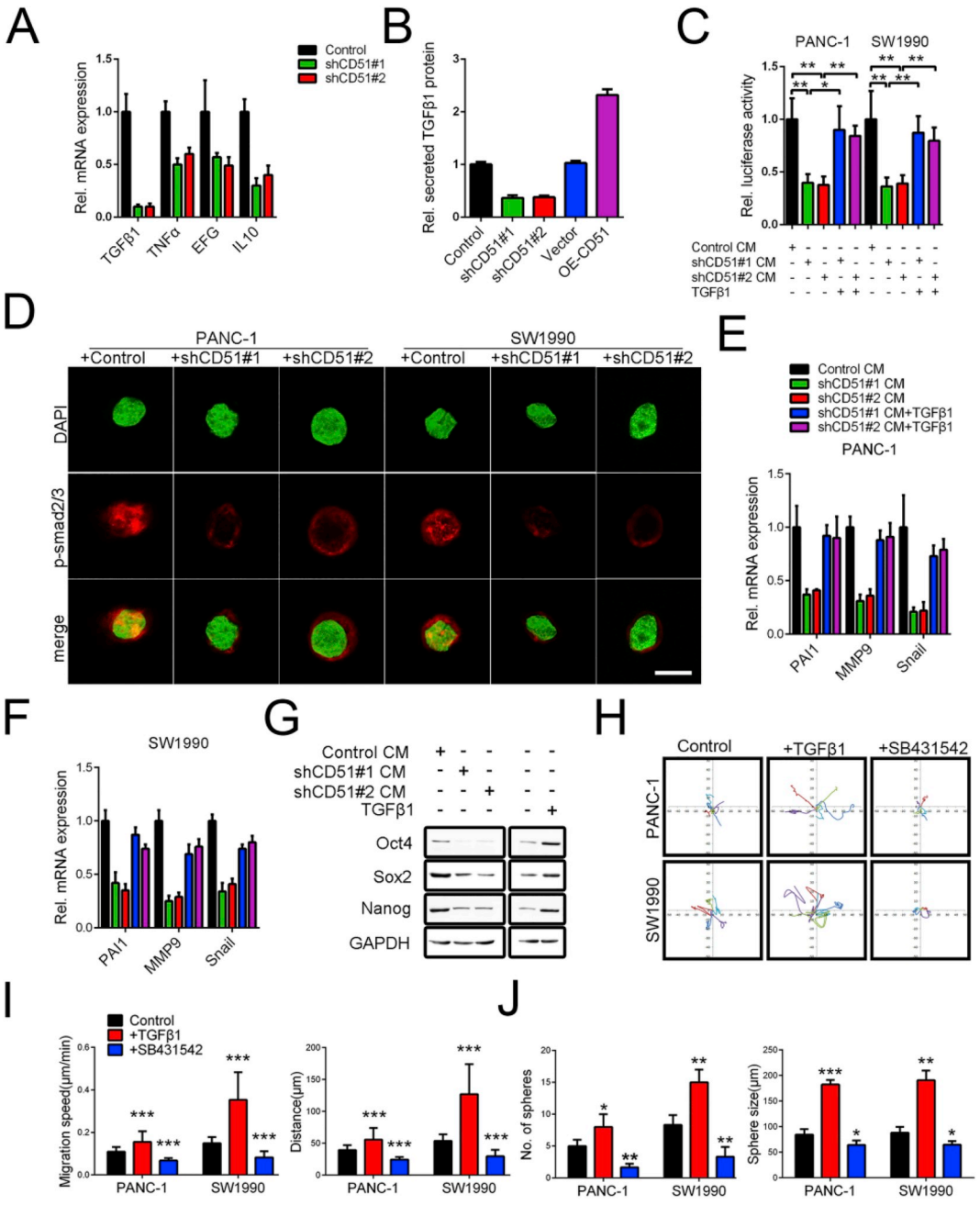

Fig. 6. CD51 promotes macrophage TGFβ1 expression to enhance CSC phenotypes.

A. The expression of macrophage-secreted cytokines TGFβ1, TNF-α, EFG, and IL10 was assessed by qRT-PCR.

B. The relative levels of secreted TGF-β1 protein were increased in macrophages treated with OE-CD51 but decreased in macrophages with CD51 knockdown (*: $P < 0.05$, **: $P < 0.01$).

C. SBE luciferase reporter gene activity. After coculture with CM from the indicated macrophages, pancreatic cancer cells were transiently transfected with an SBE luciferase reporter gene, and the TGF-β1 group was stimulated with 5 ng/ml TGF-β1 for 24 h. The results were expressed as the fold change in luciferase activity with respect to that of the vector control. The error bars represent the SDs of data obtained from 3 independent experiments (**$P < 0.01$; ns, no significant difference).

D. Representative images of the immunofluorescence results for anti-P-smad2/3 (red) and DAPI (green) staining. Pancreatic cancer cells were cultured with the indicated macrophages for 2 days and were collected for immunofluorescence analysis. Scale bar, 10 μm.

E-F. The expression of TGF-β target gene was downregulated in pancreatic cancer cells treated with CD51 knockdown macrophages and was rescued by TGF-β1 treatment. The error bars represent the SDs of data obtained from 3 independent experiments.

G. The protein expression of CSC-related transcription factors was assessed.

H-I. The motility of pancreatic cancer cells treated with TGF-β1 or SB431542 (an inhibitor of the TGF-β receptor) was assessed (***: $P < 0.001$).

J. The sphere formation capacity of pancreatic cancer cells treated with TGF-β1 or SB431542 was assessed (*: $P < 0.05$, **: $P < 0.01$, ***: $P < 0.001$).

treatment with CD51 knockdown macrophages (Supplementary Fig. 5A). Transwell assays and expression analysis of EMT-related genes demonstrated that knockdown of CD51 in M2 macrophages markedly suppressed the migratory ability of PDAC cells (Fig. 3B and C, Supplementary Fig. 5B). The results of the cell motility assays were similar to those of the Transwell assays (Fig. 3G and H). Macrophage CD51 inhibition also reduced the chemoresistance of PDAC cells to gemcitabine (Supplementary Fig. 5C and D). In addition, the percentage

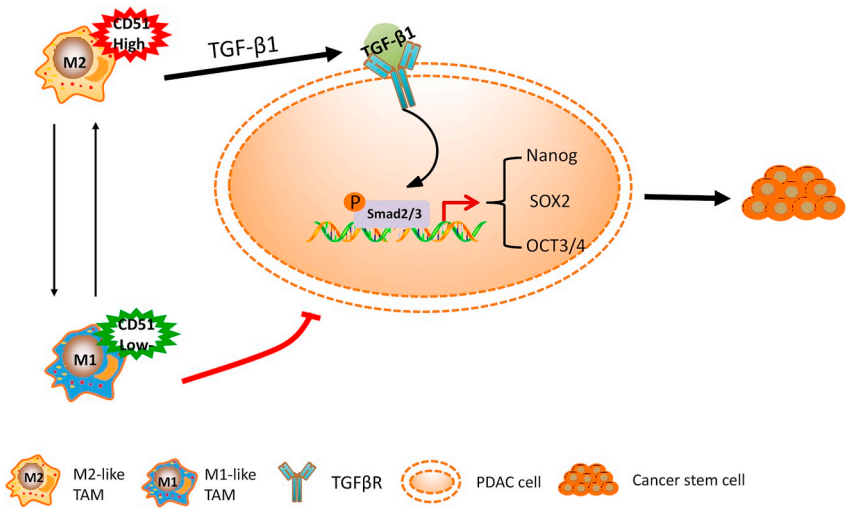

Fig. 7. Diagram of the crosstalk between CD51-high or CD51-low macrophages and pancreatic cancer cells. Macrophages with CD51 upregulation display M2-like phenotypes and secrete TGF-β1 to facilitate smad2/3 nuclear translocation followed by the activation of CSC-TFs (Nanog, Oct3/4 and Sox2). Therefore, CD51-high macrophages act as tumor promoters, which facilitate the acquisition of CSC properties of pancreatic cancer cells. In contrast, macrophages expressing lower levels of CD51 display M1-like phenotypes and act as tumor suppressors.

of CD133 + cells among pancreatic cancer cells treated with CD51 knockdown macrophages was clearly reduced (Fig. 3D and E). Moreover, the sphere-forming capacity of pancreatic cancer cells cocultured with CD51 knockdown macrophages was decreased compared with that of the control-treated groups (Fig. 3F). Consistent with a pro-CSC effect, treatment with CD51 knockdown macrophages increased the apoptosis and necrosis of pancreatic cancer cells following treatment with gemcitabine (Fig. 3I). These data suggest that macrophage-expressed CD51 facilitates PDAC tumor progression by potentiating CSC self-renewal and tumorigenesis.

3.5. Macrophage-expressed CD51 accelerates pancreatic oncogenesis in vivo

Given that CD51 knockdown in macrophages is protective in PDAC cells, we postulated that macrophage-expressed CD51 might lead to accelerated tumorigenesis *in vivo*. To test this hypothesis, we treated 4-week-old NOD/SCID mice with pancreatic cancer cells mixed with M2 macrophages as indicated and assessed tumor progression 4 weeks later. The absence of CD51 impaired tumor growth *in vivo*; both the tumor sizes and weights were significantly decreased in the group injected with shCD51 cells compared with those in the group injected with PDAC cells mixed with M2 macrophages (Fig. 4A–C). Similarly, cell proliferation was decelerated in mice injected with CD51-silenced macrophages, as measured by Ki-67 staining (Fig. 4E). Moreover, mice treated with shCD51 cells exhibited less mesenchyme, whereas mice treated with PDAC cells mixed with M2 macrophages showed denser stroma, as further evaluated by H&E staining of tumor sections (Fig. 4D; Supplementary Fig. 6A and B). In addition, the percentage of CD133 + cells in tumors formed by PDAC cells mixed with CD51 knockdown macrophages was clearly reduced (Fig. 4F). Taken together, these findings indicate that macrophage-expressed CD51 enhances CSC phenotypes both *in vitro* and *in vivo*.

3.6. CD51 induces immunogenic reprogramming of macrophages

Immune homeostasis depends on the balance between the generation of proinflammatory (M1) and anti-inflammatory (M2) macrophages, a process known as polarization. In tumors, TAMs predominately exhibit M2-type functions and diminish tumor cell killing by cytotoxic T cells and natural killer (NK) cells [20]. To determine the relationship between CD51 expression and macrophage polarization, we performed flow cytometric analysis to further assess the expression of M2-specific (CD206 and CD163) and M1-specific (HLA-DR and CD86) markers and demonstrated that CD51 knockdown decreased M2 marker expression but increased M1 marker expression in macrophages (Fig. 5A and B). Moreover, the western blotting and IHC results showed that knockdown of CD51 in macrophages reduced arginase-1 (ARG-1) expression (Fig. 5C, E). Furthermore, qRT-PCR was performed to assess the expression of IL-12, NOS2, IL1β, TGF-β1, IL10, and Arg1 as markers of M1 or M2 macrophages (Fig. 5D). To investigate the correlation of CD51 and M2 macrophages' biomarkers, we performed additional IHC in PDAC tissues. As expected, CD51 and CD206 were coexpressed in PDAC tissues (Supplementary Fig. 7A). Moreover, the analysis of correlation of CD51 with CD206 (MRC1) or CD163 showed that CD51 expression is positively correlated with CD206 (MRC1) and CD163 expression (Supplementary Fig. 7B). Taken together, these results suggest that CD51 drives macrophage polarization toward an M2-like phenotype.

3.7. Macrophage TGF-β1 expression is regulated by CD51 to promote CSC phenotypes

Because macrophage CM enhances the "stemness" of PDAC CSCs, we reasoned that CD51 might promote the secretion of pro-CSC factors by macrophages in response to cues from PDAC CSCs. To validate this hypothesis, we assessed the expression of many tumor progression-promoting cytokines secreted by macrophages, including TGF-β1, TNF-α, EFG, and IL10 [17], and confirmed that CD51 knockdown decreased the levels of these cytokines, especially TGF-β1 (Fig. 6A). As expected, overexpression of CD51 significantly promoted TGF-β1 expression in macrophages (Fig. 6B). Several studies have shown that Smad family members are the point of convergence for canonical TGF-β signaling pathways [21,22]. We performed smad-binding element (SBE) luciferase reporter gene activity assays and p-smad2/3 immunofluorescence assays to investigate the activation of the TGF-β pathway. The luciferase reporter assay results demonstrated that TGF-β1 rescued TGF-β pathway activation in pancreatic cancer cells treated with CD51 knockdown macrophages (Fig. 6C). Consistent with this finding, the immunofluorescence assay results indicated that the nuclear translocation and expression of p-smad2/3 was dramatically inhibited in PDAC cells by knockdown of macrophage-expressed CD51 (Fig. 6D). Moreover, we performed rescue experiments to determine whether macrophages contribute to CSC phenotypes through secreting TGF-β1. The qRT-PCR results showed that CD51 knockdown inhibited the expression of TGF-β target genes and that treatment with TGF-β1 partially reversed these effects (Fig. 6E and F). Consistent with these results, the protein expression of CSC-related transcription factors was rescued by treatment with TGF-β1 (Fig. 6G). In addition, the TGF-β inhibitor SB431542 reduced the motility of PDAC cells, while TGF-β1 stimulation had the opposite effect (Fig. 6H and I). Moreover, the sphere-forming capacity of PDAC cells treated with TGF-β1 was increased, while that of

PDAC cells treated with SB431542 was decreased (Fig. 6J). Collectively, these data indicate that macrophage-expressed CD51 plays a critical role in regulating the TGF-β1 expression level, which contributes to the acquisition of stemness traits of PDAC cells (Fig. 7).

4. Discussion

Macrophages are one of the most dynamic stromal cells in pancreatic cancer, which is characterized by immune tolerance and immunotherapeutic resistance [23–25]. Interestingly, macrophages are confirmed to have paradoxical roles in tumors—on the one hand, suppressing tumor development (M1 macrophages); on the other hand, driving tumor progression (M2 macrophages) [16,17]. However, the regulators of macrophage polarization in PDAC and macrophage-targeted therapies remain unclear. In this study, we demonstrated that CD51 was highly expressed in primary pancreatic cancer tissues. However, CD51 was overexpressed in macrophages rather than in pancreatic cancer cells and facilitated M2-like polarization in macrophages. As shown by our results, CD51-positive TAMs drive the CSC properties of pancreatic cancer cells, partially due to paracrine induction of TGF-β1.

Resistance to cancer treatment can be intrinsic to tumor cells, but it is often conferred by nonmalignant cells that comprise the tumor microenvironment [24]. Thus, researchers have focused on strategies to target tumor stromal cells in pancreatic cancer [26]. Tissue-resident cells and a large proportion of recruited immune cells constitute the pancreatic cancer microenvironment, among which macrophages have been identified as a major population of inflammatory cells [27]. We found that PDAC cells express lower levels of CD51 than peritumoral macrophages, which express high levels of CD51. Furthermore, functional experiments in pancreatic cancer seemed to indicate that CD51 is inconsequential to tumorigenesis because neither overexpression nor knockdown of CD51 in PDAC cells influenced their proliferative and migratory properties. Regarding other stromal cells, cancer-associated fibroblasts (CAFs) are important components in pancreatic cancer due to the abundant desmoplasia. A major source of CAFs in PDAC is pancreatic stellate cells (PSCs), resident mesenchymal cells in the pancreas [28]. Horioka et al. demonstrated that stromal CD51 expression is associated with shorter patient survival times and that suppression of CD51 in pancreatic stellate cells inhibits tumor growth [29]. These findings indicate that CD51 is expressed not only on TAMs but also on CAFs and promotes pancreatic cancer progression through different mechanisms.

CD51, also called integrin αV, belongs to the integrin family. Integrins are αβ heterodimeric integral membrane proteins that mediate cell-to-extracellular matrix and cell-to-cell interactions [30]. In macrophages, α5β1 [31], β2 [32], and β3 [33] integrins have been implicated in M1 macrophage polarization, while β1 [32,34], αX [35], and α4/α9 [36] integrins play a vital role in promoting M2 macrophage polarization. Integrins αVβ3 have been proven to be involved in M2 macrophage polarization after treatment with cilengitide but not under natural conditions [37]. However, whether CD51 drives macrophage polarization remains largely unknown. In this study, we first found that CD51 regulated the M2-like polarization of macrophages under natural conditions. However, the underlying molecular mechanisms that govern the interaction between CD51 and M2 macrophage polarization deserve further exploration.

Immune homeostasis depends on the balance between the generation of proinflammatory (M1) and anti-inflammatory (M2) macrophages, a process known as polarization. TAMs predominantly exhibit M2-type functions and diminish tumor cell killing by cytotoxic T cells and NK cells [20]. TAMs promote cancer initiation and malignant progression by stimulating angiogenesis; increasing tumor cell migration, invasion, and intravasation; and suppressing antitumor immunity [24]. In pancreatic cancer, macrophages have been reported to promote CSC phenotypes [18,19]. However, most studies have focused on proteins secreted from macrophages, such as ISG5, hCAP-18/LL-37, or on the chemotactic factor and receptor-like CCR2 protein [38]. In this study, we focused on macrophage membrane proteins and demonstrated that CD51-positive TAMs facilitated the development of pancreatic CSC phenotypes.

M2-type macrophages play a central role in tumor propagation [39]. M2-type macrophages drive tumor development through secreted proteins such as TGF-β, TNF-α, and EGF, which promote tumor invasiveness, and TGF-β, PD-L1, IL10, IL4, and IL13, which promote immunosuppression [17]. We measured the expression levels of these important secretory factors and found that after CD51 inhibition, the expression of TGF-β1 was the most significantly reduced. Further experiments showed that macrophage-expressed CD51 increased TGF-β1 secretion, which activated the smad2/3 pathway and increased the expression of stemness-related transcription factors (Nanog, Sox2 and Oct4) in pancreatic cancer cells.

In conclusion, we demonstrated that CD51-high TAMs play an important role in malignant biological behavior and facilitate the acquisition of stemness traits of pancreatic cancer cells, partially due to paracrine secretion of TGF-β1. Our work provides the first connection between the CD51/TGF-β1/smad2/3 axis and PDAC CSC properties. Further studies could focus on the mechanism by which CD51 expression is increased on TAMs in pancreatic cancer. Our data not only advance the understanding of the role of TAMs in pancreatic cancer but also shed new light on future applications for targeting CD51 in cancer therapy, particularly approaches focused on reprogramming the protumoral activities of TAMs.

Conflicts of interest

The authors declare no conflicts of interest.

Funding sources

This work was supported by the National Natural Science Foundation of China [grant numbers 81871945, 81702951, 81672395, 81672807, 81370059, 81000917, 81702417, and 81402213; www.nsfc.gov.cn], the Guangdong Science and Technology Department [grant numbers S2012010008934, 2014A030313044, 2014A030311047, 2016A030313340, 2016A030313296, 2017A030313880, and 2017B030314026; http://pro.gdstc.gov.cn], the China Postdoctoral Science Foundation Grant [grant number 2018M643346] and the Sun Yat-sen University Clinical Research Foundation of 5010 Project [grant number 2012007].

Author contributions

B. Z., H. Y., X.R., Z.L. and R.C. designed and performed the experiments. B. Z., H. Y. and X.R. analyzed the results. B. Z., H. Y. and X.R. organized the results and wrote the paper. S.Z, Q.Z, C.C, Q.L., G.L., L.W., Z.F. C.H. and Y. Z. provided the tools and patient specimens and edited the manuscript. All authors participated in critical revision of the manuscript for important intellectual content.

Patient consent

Obtained.

Ethics approval

Studies using human PDAC tissue samples were approved by the ethics committee of Sun Yat-sen Memorial Hospital of Sun Yat-sen University. The protocols for the animal studies were approved by the Institutional Animal Care and Use Committee and Institutional Biosafety Committee of Sun Yat-sen University.

Acknowledgments

The authors thank Dongxin Lin and Jian Zheng for excellent technical assistance and experimental support. The authors thank Elsevier Webshop for providing Elsevier Language Editing Services to assist with manuscript writing.

Appendix A. Supplementary data

Supplementary data to this article can be found online at https://doi.org/10.1016/j.canlet.2019.06.005.

References

[1] R.L. Siegel, K.D. Miller, A. Jemal, Cancer statistics, CA A Cancer J. Clin. 68 (2018) (2018) 7–30.
[2] L. Rahib, B.D. Smith, R. Aizenberg, A.B. Rosenzweig, J.M. Fleshman, L.M. Matrisian, Projecting cancer incidence and deaths to 2030: the unexpected burden of thyroid, liver, and pancreas cancers in the United States, Cancer Res. 74 (2014) 2913–2921.
[3] M. Liu, J. Yang, Y. Zhang, Z. Zhou, X. Cui, L. Zhang, et al., ZIP4 promotes pancreatic cancer progression by repressing ZO-1 and claudin-1 through a ZEB1-dependent transcriptional mechanism, Clin. Cancer Res. 24 (2018) 3186–3196.
[4] J. Yang, Z. Zhang, Y. Zhang, X. Ni, G. Zhang, X. Cui, et al., ZIP4 promotes muscle wasting and cachexia in mice with orthotopic pancreatic tumors by stimulating RAB27B-regulated release of extracellular vesicles from cancer cells, Gastroenterology 156 (2019) 722–734 e6.
[5] J.E. Visvader, G.J. Lindeman, Cancer stem cells in solid tumours: accumulating evidence and unresolved questions, Nat. Rev. Canc. 8 (2008) 755–768.
[6] R.O. Hynes, Integrins: bidirectional, allosteric signaling machines, Cell 110 (2002) 673–687.
[7] J. Wang, B. Zhang, H. Wu, J. Cai, X. Sui, Y. Wang, et al., CD51 correlates with the TGF-beta pathway and is a functional marker for colorectal cancer stem cells, Oncogene 36 (2017) 1351–1363.
[8] X. Sui, J. Cai, H. Li, C. He, C. Zhou, Y. Dong, et al., p53-dependent CD51 expression contributes to characteristics of cancer stem cells in prostate cancer, Cell Death Dis. 9 (2018) 523.
[9] A. Saalbach, A. Wetzel, U.F. Haustein, M. Sticherling, J.C. Simon, U. Anderegg, Interaction of human Thy-1 (CD 90) with the integrin alphavbeta3 (CD51/CD61): an important mechanism mediating melanoma cell adhesion to activated endothelium, Oncogene 24 (2005) 4710–4720.
[10] H. Jin, Y. He, P. Zhao, Y. Hu, J. Tao, J. Chen, et al., Targeting lipid metabolism to overcome EMT-associated drug resistance via integrin beta3/FAK pathway and tumor-associated macrophage repolarization using legumain-activatable delivery, Theranostics 9 (2019) 265–278.
[11] L. Schleier, M. Wiendl, K. Heidbreder, M.T. Binder, R. Atreya, T. Rath, et al., Non-classical monocyte homing to the gut via alpha4beta7 integrin mediates macrophage-dependent intestinal wound healing, Gut (2019), https://doi.org/10.1136/gutjnl-2018-316772 gutjnl-2018-316772.
[12] M.M. Kaneda, K.S. Messer, N. Ralainirina, H. Li, C.J. Leem, S. Gorjestani, et al., PI3Kgamma is a molecular switch that controls immune suppression, Nature 539 (2016) 437–442.
[13] P. Foubert, M.M. Kaneda, J.A. Varner, PI3Kgamma activates integrin alpha4 and promotes immune suppressive myeloid cell polarization during tumor progression, Cancer Immunol Res 5 (2017) 957–968.
[14] W. Zhou, S.Q. Ke, Z. Huang, W. Flavahan, X. Fang, J. Paul, et al., Periostin secreted by glioblastoma stem cells recruits M2 tumour-associated macrophages and promotes malignant growth, Nat. Cell Biol. 17 (2015) 170–182.
[15] Z. Tang, C. Li, B. Kang, G. Gao, C. Li, Z. Zhang, GEPIA: a web server for cancer and normal gene expression profiling and interactive analyses, Nucleic Acids Res. 45 (2017) W98–W102.
[16] A. Mantovani, F. Marchesi, A. Malesci, L. Laghi, P. Allavena, Tumour-associated macrophages as treatment targets in oncology, Nat. Rev. Clin. Oncol. 14 (2017) 399–416.
[17] C. Ngambenjawong, H.H. Gustafson, S.H. Pun, Progress in tumor-associated macrophage (TAM)-targeted therapeutics, Adv. Drug Deliv. Rev. 114 (2017) 206–221.
[18] B. Sainz, S. Alcala, E. Garcia, Y. Sanchez-Ripoll, M.M. Azevedo, M. Cioffi, et al., Microenvironmental hCAP-18/LL-37 promotes pancreatic ductal adenocarcinoma by activating its cancer stem cell compartment, Gut 64 (2015) 1921–1935.
[19] B. Sainz, B. Martin, M. Tatari, C. Heeschen, S. Guerra, ISG15 is a critical microenvironmental factor for pancreatic cancer stem cells, Cancer Res. 74 (2014) 7309–7320.
[20] H. Wang, D.J. Mooney, Biomaterial-assisted targeted modulation of immune cells in cancer treatment, Nat. Mater. 17 (2018) 761–772.
[21] J.A. Brown, Y. Yonekubo, N. Hanson, A. Sastre-Perona, A. Basin, J.A. Rytlewski, et al., TGF-β-Induced quiescence mediates chemoresistance of tumor-propagating cells in squamous cell carcinoma, Cell Stem Cell 21 (2017) 650–664 e8.
[22] C. Bellomo, L. Caja, A. Moustakas, Transforming growth factor β as regulator of cancer stemness and metastasis, Br. J. Canc. 115 (2016) 761–769.
[23] P.A. Philip, Targeting macrophages to treat pancreatic cancer, Lancet Oncol. 17 (2016) 552–553.
[24] L. Cassetta, J.W. Pollard, Targeting macrophages: therapeutic approaches in cancer, Nat. Rev. Drug Discov. 17 (2018) 887–904.
[25] S.K. Biswas, A. Mantovani, Macrophage plasticity and interaction with lymphocyte subsets: cancer as a paradigm, Nat. Immunol. 11 (2010) 889–896.
[26] Y. Komohara, M. Takeya, CAFs and TAMs: maestros of the tumour microenvironment, J. Pathol. 241 (2017) 313–315.
[27] A. Neesse, H. Algül, D.A. Tuveson, T.M. Gress, Stromal biology and therapy in pancreatic cancer: a changing paradigm, Gut 64 (2015) 1476–1484.
[28] D. Öhlund, A. Handly-Santana, G. Biffi, E. Elyada, A.S. Almeida, M. Ponz-Sarvise, et al., Distinct populations of inflammatory fibroblasts and myofibroblasts in pancreatic cancer, J. Exp. Med. 214 (2017) 579–596.
[29] K. Horioka, K. Ohuchida, M. Sada, B. Zheng, T. Moriyama, H. Fujita, et al., Suppression of CD51 in pancreatic stellate cells inhibits tumor growth by reducing stroma and altering tumor-stromal interaction in pancreatic cancer, Int. J. Oncol. 48 (2016) 1499–1508.
[30] H. Hamidi, J. Ivaska, Every step of the way: integrins in cancer progression and metastasis, Nat. Rev. Canc. 18 (2018) 533–548.
[31] S.J. Lee, C.K. Lee, S. Kang, I. Park, Y.H. Kim, S.K. Kim, et al., Angiopoietin-2 exacerbates cardiac hypoxia and inflammation after myocardial infarction, J. Clin. Investig. 128 (2018) 5018–5033.
[32] L. Lv, Y. Xie, K. Li, T. Hu, X. Lu, Y. Cao, et al., Unveiling the mechanism of surface hydrophilicity-modulated macrophage polarization, Adv. Healthc. Mater. 7 (2018) e1800675.
[33] S. Ferguson, S. Kim, C. Lee, M. Deci, J. Nguyen, The phenotypic effects of exosomes secreted from distinct cellular sources: a comparative study based on miRNA composition, AAPS J. 20 (2018) 67.
[34] R. Li, J.C. Serrano, H. Xing, T.A. Lee, H. Azizgolshani, M. Zaman, et al., Interstitial flow promotes macrophage polarization toward an M2 phenotype, Mol. Biol. Cell 29 (2018) 1927–1940.
[35] Y.H. Zheng, Y.Y. Deng, W. Lai, S.Y. Zheng, H.N. Bian, Z.A. Liu, et al., Effect of bone marrow mesenchymal stem cells on the polarization of macrophages, Mol. Med. Rep. 17 (2018) 4449–4459.
[36] T. Kobori, S. Hamasaki, A. Kitaura, Y. Yamazaki, T. Nishinaka, A. Niwa, et al., Interleukin-18 amplifies macrophage polarization and morphological alteration, leading to excessive angiogenesis, Front. Immunol. 9 (2018) 334.
[37] Q. Yao, J. Liu, Z. Zhang, F. Li, C. Zhang, B. Lai, et al., Peroxisome proliferator–activated receptor γ (PPARγ) induces the gene expression of integrin αVβ5 to promote macrophage M2 polarization, J. Biol. Chem. 293 (2018) 16572–16582.
[38] J.B. M, D.J. B, B.L. K, B.A. B, Y. Z, D.E. S, et al., Targeting tumor-infiltrating macrophages decreases tumor-initiating cells, relieves immunosuppression, and improves chemotherapeutic responses, Cancer Res. 73 (2013) 1128–1141.
[39] H. Ye, Q. Zhou, S. Zheng, G. Li, Q. Lin, L. Wei, et al., Tumor-associated macrophages promote progression and the Warburg effect via CCL18/NF-kB/VCAM-1 pathway in pancreatic ductal adenocarcinoma, Cell Death Dis. 9 (2018) 453.